

# Hybrid Adaptive Channel Estimation Technique in Time and Frequency Domain for MIMO-OFDM Systems

S.B. Lenin, N. Tamilarasan, S. Malarkkan

**Abstract---** A multiple-input multiple (MIMO) communication model is integrated to orthogonal frequency division multiplexing (OFDM) for reliable and data transmission at a higher rate in the broadband wireless channels. A significant part in the wireless data transmission is use of adaptive channel estimation techniques in which the channel is frequently varying. This paper introduces a hybrid adaptive channel estimation technique by integrating the beneficial characteristics of the time domain as well as frequency domain. The column based time domain and the row based frequency domain are combined together and they are used based on the channel quality and received bit error rate (BER). Here, the channel estimation at pilot frequencies depends on minimum mean square error (MMSE). For the evaluation of the proposed techniques, a set of experiments and detailed comparative analysis is made interms of different measures under different condition. The experimental results depicted the proposed method outperforms the other methods.

**Keywords---** Channel estimation, OFDM, CSI, MMSE.

## I. INTRODUCTION

Adaptive resource allocation using the channel state information (CSI) received more attention of improving data rate by achieving high quality of service in time-varying wireless channels [1]–[4]. So, the adaptive modulation is introduced in which the rate of data transmission and power are altered using perfect CSI at the transmitter which indicates the results are enhanced when compared to static wireless communication through flat fading channels [5]–[6]. In the meantime, frequency selection in the wireless channel will be inevitable in case of an increase in transmission symbol rate. OFDM is an efficient method which uses the concept by transforming a frequency selective fading channel to a collection of closely flat narrowband orthogonal fading channels; hence the simplified equalization is attained at the receiver [7]. The main benefits of adaptive modulation techniques used on precise CSI were assumed for multiple carrier system [3], [8]. Several works on adaptive modulation indicated that there is an assumption of proper CSI present at the transmitter side. However, it is impossible for the perfect CSI at the transmitter because of time variations in the channel and improper channel estimation due to noise. The impact of improper channel estimation on the results of adaptive modulation using precise CSI at the transmitter is investigated and depicted high sensitivity to bit error rate (BER) for channel estimation error as well the variations

in the channel. So, adaptive modulation techniques should be considered for the use of improper CSI at the transmitter [9]–[14].

Channel sounding by the use of pilot symbol assisted modulation (PSAM) [15]–[17] in which the pilot symbols are appended in a particular time interval while transmitting the sequence rather than inserting a long training sequence in prior to the transmission of the signal, is an efficient model for channel estimation and prediction in fast fading environment. The two kinds of fundamental channel estimation methods in OFDM are block type and comb type pilot-based channel estimation. The former type allocates the pilot signal to specific OFDM block and transmits it periodically in the time domain. The latter type distributes the pilot signals uniformly in every OFDM block. The comb pilot-based channel estimation uses algorithm for estimating the channel at the pilot frequencies and interpolates the channel at data frequencies. The channel estimation at pilot frequencies depends on least square (LS), minimum mean square error (MMSE), zero forcing (ZF) or least mean square (LMS) method, while different interpolation techniques can be incorporated for the channel estimation at data frequencies [18, 19]. On the other hand, as pilot symbol does not carry information, it still consumes a significant amount of energy and the insertion of pilots produces an overhead in the transmission model. Hence, an effective model should consider the optimal usage of pilots and adaptive systems. An adaptive PSAM technique is presented in [11] to optimize the pilot parameters for single carrier transmission using imperfect CSI. To overcome the limitations of the existing techniques, this paper presents a novel, hybrid adaptive channel estimation technique by integrating the beneficial characteristics of the time domain as well as frequency domain. The column based time domain and the row based frequency domain are combined together and they are used based on the channel quality. The channel estimation at pilot frequencies depends on minimum mean square error (MMSE). For the evaluation of the proposed techniques, a set of experiments and detailed comparative analysis is made interms of different measures under different conditions. The experimental results depicted the proposed method outperforms the other methods.

The paper organization is given as follows: Next section deals with the system model of a wireless MIMO-OFDM communication system in time domain and frequency domain.

**Revised Version Manuscript Received on 22 February, 2019**

**S.B. Lenin**, Research Scholar, Sathyabama University, Tamil Nadu, India. (e-mail: lenin.ram@gmail.com)

**N. Tamilarasan**, Research Scholar, Pondicherry University, Tamil Nadu, India. (e-mail: neithalarasu@gmail.com)

**S. Malarkkan**, Principal, Manakular Vinayagar Institute of Technology, Pondicherry, India. (e-mail: malarkkan\_s@yahoo.com)

Section 3 explains the presented method and the results are analyzed in Section 4. At the end, section 5 concludes the paper.

## II. SYSTEM MODEL

In this paper, we consider synchronization of perfect timing and perfect channel estimation together. Fig. 1 shows the overall system model employed in this study. Initially, the input from the source will be modulated and it is converted by the use of S/P. Then, the pilots are inserted adaptively and then IDFT takes place. Next, the guard bits are inserted to avoid overlapping of data. Then, they are converted back to serial data and are transmitted to the destination. At the receiving side, initially S/P conversion takes place and then guard bits are removed which are included at the transmitter side. Then the demodulation, i.e. DFT takes place. Then, the hybrid channel estimation takes (frequency and time domain) by the use of demodulated data and reference pilot signals. Then, the interference will be cancelled and the signals are detected by the detector. The detected signals are sent back for effective channel prediction and channel estimation. Finally, the P/S again takes place and the signal will be demodulated.

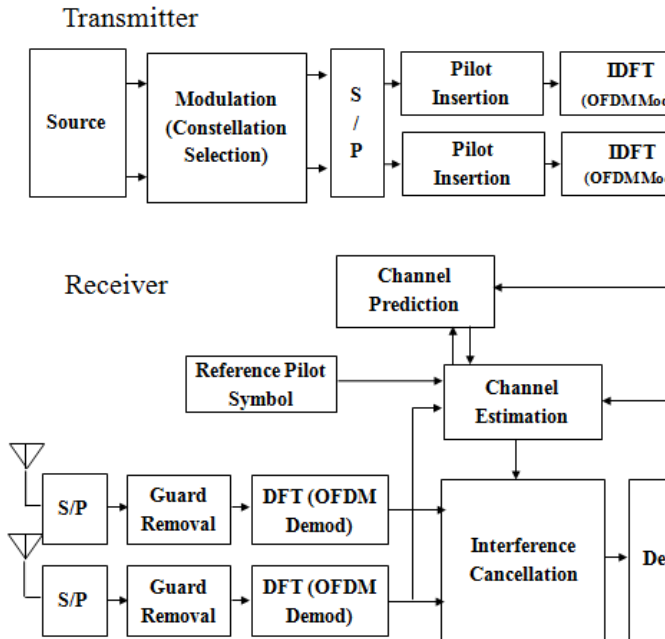


Fig. 1: Overall system model

With  $N_r$  receive and  $N_t$  transmit antennas, assume an OFDM depended MIMO communication system which is wireless. By the below expression, the transmitted time domain signal can be demonstrated.

$$s_{j,i} = \frac{1}{N_c} \sum_{n=0}^{N_c-1} S_{j,n} e^{\frac{2\pi n i}{N_c}} \quad (1)$$

Where  $S_{j,n}$  is the symbol sent to the  $j$ th antenna and  $n$ th subcarrier and belongs to the constellation  $S$  with size  $|S| = 2m$ ,  $m$  is the modulation order,  $i = 0 \sim N_c - 1$ ,  $j = 0 \sim N_t - 1$ ,  $N_c$  is the FFT size,  $s_{j,i}$  is the  $i$ th sample of the time domain signal transmitted on the  $j$ th antenna. The cyclic prefix vector can be demonstrated as:

$$\tilde{s}_{CP,j}(i) = s_j, N_c - N_G - N_G + i \quad (2)$$

where  $i = 0 \sim N_c - 1$ ,  $N_G$  is the guard interval length. The  $i$ th sample of the received time domain signal at the  $k$ th antenna might be equated as:

$$y_{k,i} = \sum_{j=0}^{N_t-1} \sum_{l=0}^{N_c} h_{k,j,l}^{(i)} s_{j,((i-l))_{N_c}} + z_{k,i} \quad (3)$$

where  $i = 0 \sim N_c - 1$ ,  $k = 0 \sim N_r - 1$ ,  $h_{k,j,l}^{(i)}$  is the  $l$ th channel tap gain among  $k$ th receive antenna and the  $j$ th transmit antenna,  $((\cdot))_{N_c}$  indicates a cyclic shift in the base of  $N_c$  and  $z_{k,i}$  is a sample of AWGN noise with zero mean and variance  $\sigma_z^2$ . After, in frequency domain, the channel coefficients can be written as:

$$H_{k,j,n}^d = \frac{1}{N_c} \sum_{l=0}^{N_c} F_l(d) e^{-j \frac{2\pi l(n-d)}{N_c}} \quad (4)$$

$$H_{k,j,n}^d = \frac{1}{N_c} \sum_{l=0}^{N_c} \sum_{i=0}^{N_c-1} h_{k,j,l}^{(i)} e^{-j \frac{2\pi l(n-d)}{N_c}} = \sum_{l=0}^{N_c} h_{k,j,l}^{ave} e^{-j \frac{2\pi l n}{N_c}} \quad (5)$$

where  $n, d = 0 \sim N_c - 1$ ,  $h_{k,j,l}^{ave}$  is average of the  $l$ th channel tap. Without loss of generality, only the  $n$ th subcarrier of the MIMO-OFDM receiver is assumed. Eq.(4) can be reformulated as:

$$Y_n = H_n^0 S_n + \sum_{d=1}^{N_c-1} H_n^d S_{((n-d))_{N_c}} + Z_n \quad (6)$$

Where  $Y_n \equiv (Y_{0,n}, \dots, Y_{(N_r-1),n})^T$ ,  $H_n^0 \equiv \{H_{k,j,n}^0\}$  and  $H_n^d \equiv \{H_{k,j,n}^d\}$  are together  $N_r \times N_t$  channel matrices,  $S_n \equiv (S_{0,n}, \dots, S_{(N_t-1),n})^T$ ,  $Z_n \equiv (Z_{0,n}, \dots, Z_{(N_r-1),n})^T$ ,  $Z_{k,n}$  is an i.i.d. complex Gaussian noise with zero mean and variance  $\sigma_z^2$ . Furthermore, the input data of the  $n$ th subcarrier as a binary  $m \times N_t$ -vector,  $b_n \equiv (b_0, \dots, b_{N_t-1,n})^T$ , where  $b_n \equiv (b_{j,0}, \dots, b_{j,m-1})$  and  $b_{j,q} \in \{0, 1\}$ . The binary data vector  $b_n$  is mapped to the symbol vector  $S_n$ .

## III. PROPOSED HYBRID ADAPTIVE CHANNEL ESTIMATION MODEL

A novel hybrid adaptive channel estimation technique is introduced by integrating the beneficial characteristics of the time domain as well as frequency domain. The row based frequency domain involves less complexity at the cost of slightly degraded performance. But, the column based time domain offers higher performance but with the cost of high complexity. So, in this paper, we integrate the benefits of the time domain and frequency domain for channel estimation. At the initial stage, by default, the time domain based channel estimation is employed. In case of better channel quality and attained low BER for a predefined time period, then a swapping of frequency domain from time domain takes place. Similarly, when the channel quality becomes worse and the BER is increased, an inverse swapping of frequency domain to time domain takes place. This adaptive swapping nature of both the time and frequency will helps to adaptively approximate the channel quality in an effective way. The proposed hybrid model investigated the feature of fading channels and the estimates the channel in time as well as frequency domain. Here, it is estimated that the CIR  $h_t(l)$  as a linear function of the time variable  $t$ ,

$$h_t(l) = u_0(l) + t u_1(l) \quad (7)$$

where  $u_0(l)$  and  $u_1(l)$  are the parameters to be estimated. Under varying channel conditions with a channel length  $L$ , it is needed to estimate  $2L$  parameters for every burst and



needs to be estimated for each burst, and the CIR of one burst can be computed easily using the parameters. The sample  $y_t$  received at time  $t$  can be defined as

$$y_t = x_t(u_0 + t.u_1) + n_t \quad (8)$$

where  $x_t = x_t, x_{t-1}, \dots, x_{t-L+1} \in \mathbb{C}^{1 \times L}$  are the transmitted symbols, and  $u_m = [u_m(0), u_m(1), \dots, u_m(L-1)]^T \in \mathbb{C}^{1 \times L}$ , for  $m = 0, 1$ , with  $(\cdot)^T$  indicates the transpose function. Using the known training symbols sent at the starting and ending of every burst, the received samples  $y$  using the training symbols can be represented in a matrix format as given below

$$y = A.u_0 + T.A.u_1 + n \quad (9)$$

$$= [A \ T \ A] \begin{bmatrix} u_0 \\ u_1 \end{bmatrix} + n \quad (10)$$

Where

$$y = [y_{L-1} \dots y_{15} y_{132+L-1} \dots y_{147}]^T \in \mathbb{C}^{(34-2L) \times 1} \quad (11)$$

$$n = [n_{L-1} \dots n_{15} n_{132+L-1} \dots n_{147}]^T \in \mathbb{C}^{(34-2L) \times 1} \quad (12)$$

$$A = \begin{bmatrix} x_{L-1} & x_{L-2} & \dots & x_1 & x_0 \\ \vdots & \vdots & \vdots & \vdots & \vdots \\ x_{15} & x_{14} & \dots & x_{15-L+2} & x_{15-L+1} \\ x_{132+L-1} & x_{132+L-2} & \dots & x_{133} & x_{132} \\ \vdots & \vdots & \vdots & \vdots & \vdots \\ x_{147} & x_{146} & \vdots & x_{147-L+2} & x_{147-L+1} \end{bmatrix} \in \mathbb{C}^{(34-2L) \times L} \quad (13)$$

and  $T$  is a diagonal matrix indicated by

$$T = \text{diag}\{L-1, \dots, 14, 15, 132+L-1, \dots, 146, 147\} \quad (14)$$

The cost function for an LS criterion can be defined as follows:

$$J_{LS} = (y - \Phi u)^H (y - \Phi u) \quad (15)$$

where  $\Phi = [A \ T \ A]$ ,  $u = [u_0^T \ u_1^T]^T$  and  $(\cdot)^H$  is the Hermitian transpose operator.

MMSE estimator [30] that minimizes the mean-squared error can be defined by

$$X^{(t)} = \mathcal{H}^{(t)H} (R_{WW} + \mathcal{H}^{(t)} \mathcal{H}^{(t)H})^{-1} R \quad (16)$$

Where  $R_{WW} = E[WW^T]$  is the autocorrelation matrix of AWGN vector  $W$ . The ZF estimator can be represented as

$$X^{(t)} = \mathcal{H}^{(t)H} (\mathcal{H}^{(t)} \mathcal{H}^{(t)H})^{-1} R \quad (17)$$

The MMSE reduces the square error in case of channel noise is and it becomes the ZF solution in case of the absence of noise. So, the results of the ZF and MMSE are identical in case of high. In addition, the MMSE provides better results when the SNR is low. The  $\hat{u}$ , reduced  $J_{LS}$  can be attained from the equation  $\frac{\partial J_{LS}}{\partial u^H} = 0$  and the solution is

$$\hat{u} = \begin{bmatrix} A^H A & A^H T A \\ A^H T A & A^H T^2 A \end{bmatrix}^{-1} \begin{bmatrix} A^H y \\ A^H T y \end{bmatrix} \quad (18)$$

where  $\Psi = \Phi_H \Phi$ . Here, an iterative process will be carried out for the determination of  $\hat{u}$  and it eliminates the determination of the matrix inversion  $\Psi^{-1}$ . And,  $y_i$  and  $y_j$  are the  $i$ th and  $j$ th component of the row and column vector  $x$  and  $y$  respectively. Using the above Eqs., the  $i$ th and  $j$ th received sample of  $y$  is expressed by

$$y_i = \Phi_i u + n_i \text{ for } i = 1, 2, \dots, (34-2L) \quad (19)$$

$$y_j = \Phi_j u + n_j \text{ for } j = 1, 2, \dots, (34-2L) \quad (20)$$

Where,  $\Phi_i \in \mathbb{C}^{1 \times 2L}$  and  $\Phi_j \in \mathbb{C}^{1 \times 2L}$  is the  $i$ th row and column of the matrix  $\Phi$ . The estimation of  $i$  and  $j$ , i.e. rows and columns are almost identical. The computed  $\hat{u}$  at index  $i$ , called  $\hat{u}(i)$  can be determined by the minimization of the residual sum of squares represented by  $J(i) = \sum_{j=1}^i [y_j -$

$\Phi_j u]^* [y_j - \Phi_j u]$  and  $(\cdot)^*$  is the complex conjugate. Hence, the computed  $\hat{u}(i)$  is calculated by as

$$\hat{u}(i) = [\sum_{j=1}^i \Phi_j^H \Phi_j]^{-1} [\sum_{j=1}^i \Phi_j^H y_j] \quad (21)$$

where  $\Psi(i) = \sum_{j=1}^i \Phi_j^H \Phi_j \in \mathbb{C}^{2L \times 2L}$  is a non-negative definite correlation matrix. For ensuring the correlation matrix  $\Psi(i)$  is always positive definite, and nonsingular, it is defined that  $\Psi(0) = cI$  where  $c$  is a small positive constant and  $I \in \mathbb{C}^{2L \times 2L}$  is the identity matrix; therefore, every element on the main diagonal of correlation matrix  $\Psi(i)$  is included to a small positive constant  $c$  [17]. Here, by the use of matrix-inversion lemma, the inverse of matrix  $\Psi(i)$  can be determined in an iterative manner

$$\Psi(i) = \Phi_i^H \Phi_i + \Psi(i-1) \quad (22)$$

$$\Psi^{-1}(i) = \Psi^{-1}(i-1) - \frac{\Psi^{-1}(i-1) \Phi_i^H}{1 + \Phi_i \Psi^{-1}(i-1) \Phi_i^H} \Phi_i \Psi^{-1}(i-1) =$$

$$\Psi^{-1}(i-1) - \mathcal{K}(i) \Phi_i \Psi^{-1}(i-1) \quad (23)$$

Where  $\mathcal{K}(i) = \left( \frac{\Psi^{-1}(i-1) \Phi_i^H}{1 + \Phi_i \Psi^{-1}(i-1) \Phi_i^H} \right) \in \mathbb{C}^{2L \times 1}$  is the gain vector. Finally, the computed  $\hat{u}(i)$  can be defined as

$$\begin{aligned} \hat{u}(i) &= [\Psi^{-1}(i-1) - \kappa(i) \Phi_i \Psi^{-1}(i-1)] \times \left[ \sum_{j=1}^{i-1} \Phi_j^H y_j + \Phi_i^H y_i \right] \\ &= \Psi^{-1}(i-1) \sum_{j=1}^{i-1} \Phi_j^H y_j + \kappa(i) \times [y_i \\ &\quad - \Phi_i \left( \Psi^{-1}(i-1) \sum_{j=1}^{i-1} \Phi_j^H y_j \right)] \\ &= \hat{u}(i-1) + \kappa(i) [y_i - \Phi_i \hat{u}(i-1)] \end{aligned} \quad (24)$$

Therefore, it is found that the inversion of the correlation matrix  $\Psi^{-1}$  in (20) got replaced by the inversion of scalar  $\{1 + \Phi_i \Psi^{-1}(i-1) \Phi_i^H\}$  in the estimation of  $u$ . While estimating the parameters  $u_0$  and  $u_1$ , the CIR of the whole burst can be easily attained. The above explanation is mainly focused on time domain and it is identical to frequency domain. It should be noted that the column elements are based on time domain and the row elements are focused on frequency domain.

#### IV. PERFORMANCE EVALUATION

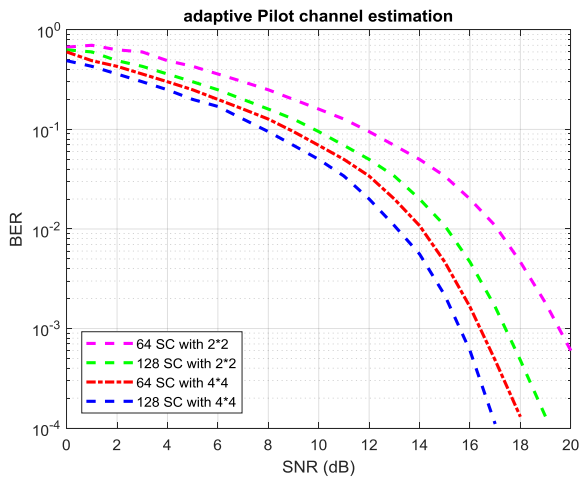
For the effective investigation on the performance of the proposed method, an extensive set of experimentation takes place under varying number of antennas, pilot, SC and mobility speed. The following parameter settings given in Table 1 are used for experimentation.

Table 1: Parameter settings

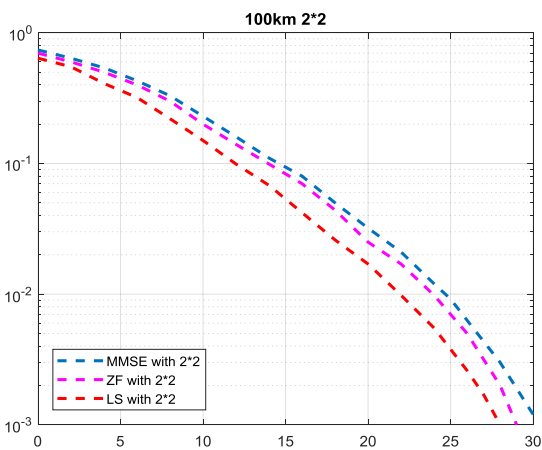
S. No	Parameters	Value
1.	Operating frequency	2.4GHz
2.	Modulation	QPSK, BPSK
3.	Estimation	ZF, MMSE, ML
4.	No. of symbols	64
5.	No. of Sub Carrier	256
6.	Channel Model	Rayleigh
7.	Antennas	2x2



Fig. 2 provides the comparative analysis of the results with different number of SC and antennas using the proposed method. From the Fig., it is obvious that the worse results are attained for less number of SC and antennas. In contrast, the results are significantly improved with more number of SC and antennas. It is verified from the figure that the BER is high for the 64SC with 2\*2 antennas and the BER is slightly reduced for the 128SC with 2\*2 antennas. In addition, it is noted that the BER is again reduced with an increase in antennas, i.e., 64 SC with 4\*4 antennas compared to 64SC with 2\*2 and 128SC with 2\*2. Here, it is noted that the increase in antenna from 2\*2 fails to attain better results compared to 4\*4. Though the number of subcarriers is low, the increase in receiving antenna from 2 to 4 has great impact on the BER. Similarly, when the transmitting antennas are also increased from 2 to 4 along with an increase in subcarriers, i.e. 128 SC with 4\*4 antennas, the maximum performance is attained with minimum BER. These observations indicated that effective results are attained for an increase in number of SC and especially number of antennas.



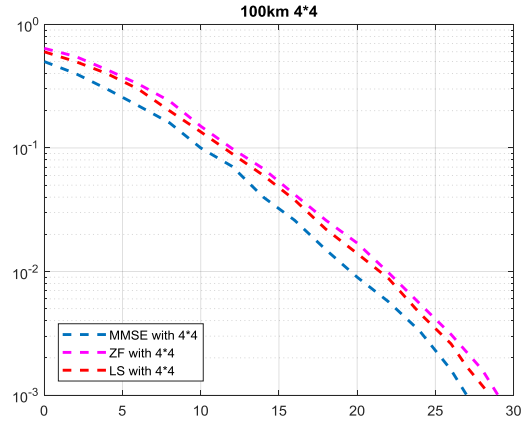
**Fig. 2: BER vs.SNR Comparison with 64 and 128 antennas**



**Fig. 3: Adaptive Channel Estimation for 100km/hr with 2\*2 antennas**

Fig. 3 shows the detailed comparative analysis of different channel estimation techniques such as MMSE, ZF and LS under varying speeds of 100km/hr. This analysis is used to validate the proposed method interms of high speed mobility. From this figure, it is clearly observed that the MMSE is not highly as efficient as ZF. Though ZF attains better results compared to MMSE under 100km/hr with 2\*2

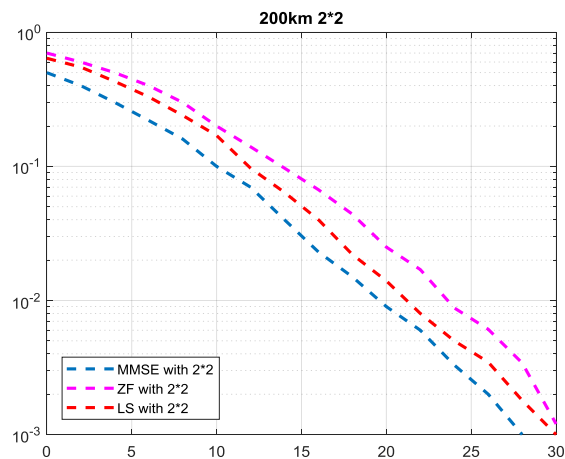
antennas, the LS shows effective performance over ZF and MMSE.



**Fig. 4: Adaptive Channel Estimation for 100km/hr with 4\*4 antennas**

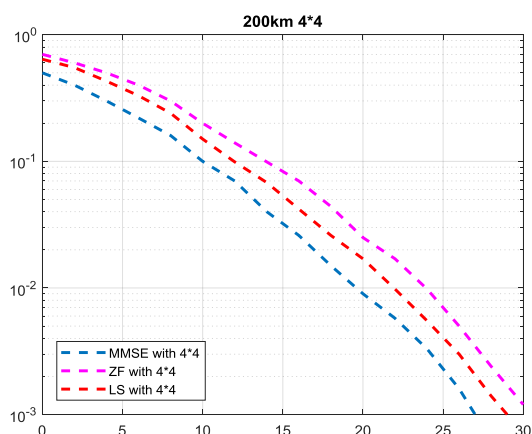
Fig. 4 depicts the performance of the proposed method under different channel estimation with a speed of 100km/hr but with the antennas of 4\*4. From the Fig., it is clear that the ZF obtains higher BER and tends to decrease to a particular point. The LS shows competitive performance with LS and leads to better results compared to ZF. And, the MMSE starts with the significantly lower BER compared to ZF and LS. It is noted that the MMSE is found to superior incase of increasing number of antennas from 2\*2 to 4\*4 under the speed of 100km/hr.

Fig. 5 depicts the results obtained by the proposed method under different channel estimation with a speed of 200km/hr. From this figure, it is apparent that the MMSE attains the lowest bit rate and the MMSE shows better performance than ZF and LS under the high mobility of 200km/hr. In addition, it is noted that the ZF shows worse performance with a highest BER whereas LS manages to maintain BER, but not outperform MMSE. It is observed that MMSE can provide better BER under 200km/hr and also with low number of antennas 2\*2.



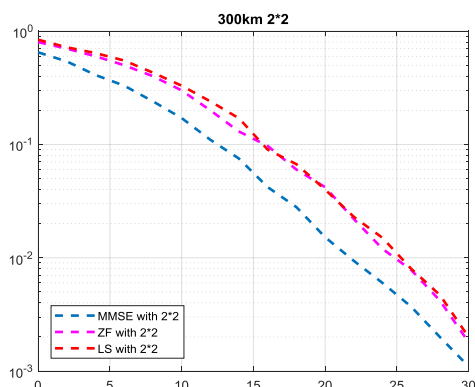
**Fig. 5: Adaptive Channel Estimation for 200km/hr with 2\*2 antennas**

Fig. 6 shows the results attained by the proposed method under different channel estimation with a speed of 200km/hr but with the increased number of antennas, i.e. 4\*4. From the Fig., it is obvious that the LS method shows poor performance with a maximum BER and fails to outperform other methods. At the same time, the LS method depicts somewhat better performance than ZF with a lower BER and it starts reducing upto a specific point. The performance of the LS is gradually better than ZF and also poor than MMSE. Furthermore, MMSE starts with the better BER compared to ZF and LS. Interestingly, MMSE maintains to achieve better results compared to other methods with an increasing number of antennas from 2\*2 to 4\*4 under the speed of 100km/hr.



**Fig. 6: Adaptive Channel Estimation for 200km/hr with 4\*5 antennas**

Though the MMSE shows better results under 100km/hr and 200km/hr, an additional investigation is needed to verify the consistent results even under high mobility, i.e. 300km/hr. Fig. 7 shows the detailed comparative analysis of different channel estimation techniques such as MMSE, ZF and LS under high mobility of 300km/hr. This analysis is used to validate the proposed method interms of high speed mobility. From this figure, it is evident that the performance of the ZF and LS are almost closer to each other and gradually increases as well as decreases at some point. At the same time, it is interesting that the MMSE is highly efficient compared to ZF and LS under 300km/hr with 2\*2 antennas. From these results, it can be seen that the MMSE is effective in case of high mobility.



**Fig. 7: Adaptive Channel Estimation for 300km/hr with 2\*2 antennas**

Fig. 8 provides the performance analysis of the proposed method under different channel estimation with a high speed of 300km/hr but with the increased number of antennas from 2\*2 to 4\*4. From the Fig., it is obvious that the ZF method shows poor performance with a maximum BER and fails to outperform other methods. At the same time, the LS method depicts somewhat better result over ZF with a lower BER and begins to reduce certainly. It is noted that MMSE maintains to achieve better results compared to other methods with an increasing number of antennas from 2\*2 to 4\*4 under the speed of 300km/hr.

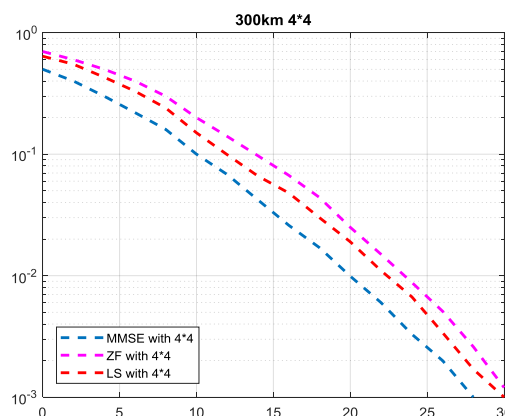


**Fig. 8: Adaptive Channel Estimation for 300km/hr with 4\*4 antennas**

From the simulation results, it is inferred that the results of MIMO-OFDM system with equalization increases the performance due to the reduction of ISI. The better improvements in the results are also due to the effective use of time domain and frequency domain adaptively in an appropriate way. It can also be inferred that the increase in number of transmitting and receiving antennas and increase in number of pilot subcarriers improve the performance due to the diversity and multiplexing gain.

## V. CONCLUSION

For adaptive resource allocation using the CSI among the transmitter and receiver side, in this paper, we have presented a hybrid adaptive channel estimation technique using the integration of time domain and frequency domain. At the initial stage, by default, the time domain based channel estimation is good. In case of better channel quality and low BER for a predefined time period, then a swapping of frequency domain from time domain takes place and vice versa. For the effective investigation on the performance of the proposed method, an extensive set of experimentation takes place under varying number of antennas, pilots, SC and mobility speed of 100-300km/hr. The better improvements in the results are also due to the effective use of time domain and frequency domain adaptively in an appropriate way. It can also be inferred that the increase in number of antennas and increase in number of pilot subcarriers increase the performance due to the diversity and multiplexing gain.

## REFERENCES

1. S. T. Chung and A. J. Goldsmith, "Degrees of freedom in adaptive modulation: a unified view," *IEEE Trans. Commun.*, vol. 49, no. 9, pp.1561–1571, 2001.
2. J. Goldsmith and S.-G. Chua, "Adaptive coded modulation for fading channels," *IEEE Trans. Commun.*, vol. 46, no. 5, pp. 595–602, 1998.
3. T. Keller and L. Hanzo, "Adaptive multicarrier modulation: a convenient framework for time-frequency processing in wireless communications," *Proc. IEEE*, vol. 88, no. 5, pp. 611–640, 2000.
4. Svensson, "An introduction to adaptive QAM modulation schemes for known and predicted channels," *Proc. IEEE*, vol. 95, no. 12, pp. 2322–2336, Dec. 2007.
5. M.-S. Alouini, X. Tang, and A. J. Goldsmith, "An adaptive modulation scheme for simultaneous voice and data transmission over fading channels," *IEEE J. Sel. Areas Commun.*, vol. 17, no. 5, pp. 837–850, 1999.
6. G. G. Raleigh and J. M. Cioffi, "Spatio-temporal coding for wireless communication," *IEEE Trans. Commun.*, vol. 46, no. 3, pp. 357–366, 1998.
7. A. Goldsmith, *Wireless Communications*. Cambridge University Press, 2005.
8. S. T. Chung and A. Goldsmith, "Adaptive multicarrier modulation for wireless systems," in *Proc. 2000 Asilomar Conf. Signals, Syst. Comput.*, vol. 2, pp. 1603–1607.
9. A. Olfat and M. Shikh-Bahaei, "Optimum power and rate adaptation for MQAM in Rayleigh flat fading with imperfect channel estimation," *IEEE Trans. Veh. Technol.*, vol. 57, no. 4, pp. 2622–2627, 2008.
10. "Optimum power and rate adaptation with imperfect channel estimation for MQAM in Rayleigh flat fading channel," in *Proc. 2005 Veh. Technol. Conf. – Fall*, vol. 4, pp. 2468–2471.
11. X. Cai and G. B. Giannakis, "Adaptive PSAM accounting for channel estimation and prediction errors," *IEEE Trans. Wireless Commun.*, vol. 4, no. 1, pp. 246–256, 2005.
12. S. Ye, R. S. Blum, and L. J. Cimini, "Adaptive OFDM systems with imperfect channel state information," *IEEE Trans. Wireless Commun.*, vol. 5, no. 11, pp. 3255–3265, 2006.
13. S. Falahati, A. Svensson, T. Ekman, and M. Sternad, "Adaptive modulation systems for predicted wireless channels," *IEEE Trans. Commun.*, vol. 52, no. 2, pp. 307–316, 2004.
14. M. Karami, A. Olfat, and N. C. Beaulieu, "Pilot symbol assisted adaptive modulation for OFDM systems with imperfect channel state information," in *Proc. 2010 IEEE Global Telecommun. Conf.*, pp. 1–6.
15. J. K. Cavers, "An analysis of pilot symbol assisted modulation for Rayleigh fading channels," *IEEE Trans. Veh. Technol.*, vol. 40, no. 4, pp. 686–693, 1991.
16. Y. Chen and N. C. Beaulieu, "Optimum pilot symbol assisted modulation," *IEEE Trans. Commun.*, vol. 55, no. 8, pp. 1536–1546, 2007.
17. S. Sampei and T. Sunaga, "Rayleigh fading compensation for QAM inland mobile radio communications," *IEEE Trans. Veh. Technol.*, vol. 42, no. 2, pp. 137–147, 1993.
18. J.H. Kotecha and A.M. Sayeed, "Transmit signal design for optimal estimation of correlated MIMO channels," *IEEE Transactions on Signal Processing*, Vol. 52, pp. 546-557, Feb. 2004.
19. C. Chuah, D.N.C. Tse, J.M. Kahn, and R.A. Valenzuela, "Capacity scaling in MIMO wireless systems under correlated fading," *IEEE Trans. on Information Theory*, Vol. 48., pp. 637-650, 2002.

